International Journal of Nanomedicine

Dovepress
open access to scientific and medical research

Open Access Full Text Article

ORIGINAL RESEARCH

Nano-hole induction by nanodiamond and nanoplatinum liquid, DPV576, reverses multidrug resistance in human myeloid leukemia (HL60/AR)

This article was published in the following Dove Press journal:
International Journal of Nanomedicine
18 July 2013
Number of times this article has been viewed

Alia Ghoneum[1,2]
Shivani Sharma[1,3]
James Gimzewski[1,3]

[1]Department of Chemistry and Biochemistry, University of California, Los Angeles, Los Angeles, [2]Department of Otalaryngology, Drew University of Medicine and Science, Los Angeles, [3]California Nanosystems Institute (CNSI) at University of California, Los Angeles, Los Angeles, CA, USA

Abstract: Recently nanoparticles have been extensively studied and have proven to be a promising candidate for cancer treatment and diagnosis. In the current study, we examined the chemo-sensitizing activity of a mixture of nanodiamond (ND) and nanoplatinum (NP) solution known as DPV576, against multidrug-resistant (MDR) human myeloid leukemia (HL60/AR) and MDR-sensitive cells (HL60). Cancer cells were cultured with different concentrations of daunorubicin (DNR) (1×10^{-9}–1×10^{-6} M) in the presence of selected concentrations of DPV576 (2.5%–10% v/v). Cancer cell survival was determined by MTT assay, drug accumulation by flow cytometry and confocal laser scanning microscopy (CLSM), and holes and structural changes by atomic force microscopy (AFM). Co-treatment of HL60/AR cells with DNR plus DPV576 resulted in the reduction of the IC_{50} to 1/4th. This was associated with increased incidences of holes inside the cells as compared with control untreated cells. On the other hand, HL60 cells did not show changes in their drug accumulation post-treatment with DPV576 and DNR. We conclude that DPV576 is an effective chemo-sensitizer as indicated by the reversal of HL60/AR cells to DNR and may represent a potential novel adjuvant for the treatment of chemo-resistant human myeloid leukemia.

Keywords: nanodiamond, nanoplatinum, daunorubicin, flow cytometry, AFM

Introduction

Nanoparticles have shown promising results for cancer therapies. Several studies have shown the success of drug delivery and cell targeting using nanoparticles.[1] One example is the conjugation of trastuzumab (Herceptin®) to doxorubicin-carrying nanoparticles which allows transport of the chemotherapeutic agent specifically to tumor cells.[2] In addition, antibody-conjugated nanoparticles have the potential to be used in active targeted drug delivery.[3] Other nanoparticles that have been studied for their use in cancer therapies include: iron oxide,[4] poly(D,L-lactide-co-glycolide)/montmorillonite,[5] poly(D,L-lactic acid),[6] nickel,[7] and human serum albumin.[2,8,9]

The development of multidrug resistance (MDR) to anticancer agents by tumor cells is a major obstacle in the chemotherapeutic cure of cancer.[10] Therefore, larger dosages of these anticancer drugs must be applied, leading to increased toxicity; side effects include myelosuppression, carcinogenic effects, alopecia, myalgia, thrombocytopenia, congestive heart failure, and immune suppression.[11–16] There are many drugs that have been shown to reverse MDR in MDR-associated protein (MRP), including: probenecid, an inhibitor of organic anion transport;[17] genistein, an inhibitor of tyrosine kinase;[18] buthionine sulfoximine, an inhibitor of glutathione synthesis;[19] ethacrynic acid to reverse glutathione S-transferase-mediated resistance; and calcium channel blockers

Correspondence: James Gimzewski
California Nanosystems Institute (CNSI), University of California, 570 Westwood Plaza, Building 114, Los Angeles, CA 90095, USA
Tel/Fax +1 310 206 7658
Email gimzewski@cnsi.ucla.edu

and calmodulin inhibitors to reverse MDR.[20] However, these agents have been shown to be toxic in humans when used at very high doses. These considerations prompted us to investigate a new modulator of MDR with lower toxicity. Earlier studies showed that a mixture of two nanoparticles – nanodiamond (ND) and nanoplatinum (NP) – in liquid form (DPV576) and in fabric form (DPV576-C), show immune modulatory effects.[21,22] In the current study, we extend our research with DPV576 to examine its chemo-sensitizing activity against DNR-resistant human myeloid leukemia (HL60/AR) in vitro.

Materials and methods

Tumor cell lines and culture conditions

Human multidrug-resistant (MDR) myeloid leukemia (HL60/AR) cells and MDR sensitive (HL60) cells were used in the present study. HL60/AR cells were kindly provided by Dr Gollapudi at the University of California (Irvine, CA, USA). HL60 cells were purchased from the American Tissue and Culture Collection (ATCC) (Manassas, VA, USA). Tumor cells were maintained in our laboratory in a complete medium (CM) that consisted of RPMI-1640, supplemented with 10% fetal calf serum (FCS), 2 mM glutamine, and 100 μg/mL streptomycin, and penicillin.

Drugs and chemicals

DNR and 3-[4,5-dimethylthiazol-2-yl]-2,5-diphenyltetrazolium bromide (MTT) were obtained from Sigma (St Louis, MO, USA). DPV576, a liquid mixture of nanodiamond (ND) and nanoplatinum (NP) solution was used. DPV576 was supplied by Venex Company (Atsugi, Kanagawa, Japan). The particle diameters of NP and ND were 10–20 nm and 100–200 nm, respectively and their final concentrations were 50 ng/mL NP and 5 μg/mL ND.

Drug sensitivity assay

Drug sensitivity was determined using a colorimetric MTT assay. This assay is based on the reduction of tetrazolium salt MTT by a mitochondrial dehydrogenase from a colorless to a blue-colored formazan product in viable cells that can be measured spectrometrically. The amount of formazan produced is proportional to the number of living cells. Cells (1×10^4/well) were seeded in 96-well plates and cultured in triplicate in the presence or absence of various concentrations of DPV576 (2.5%–10% v/v) and with or without selected concentrations of DNR (1×10^{-9}–1×10^{-6} M). The final volume of medium in each well after addition of DPV576 and/or DNR was 200 mL. The cultures were incubated at 37°C for 3 days, after which 50 μg of MTT was added to each well, and the cultures incubated for an additional 4 hours. The plates were centrifuged, the medium carefully removed, the formazan crystals solubilized with acid alcohol, and the plates read at 590 nm using an ELISA plate reader (Molecular Devices, Menlo Park, CA, USA). The 50% inhibitory concentration (IC_{50}) was determined as the drug concentration, which resulted in a 50% reduction in cell viability. The IC_{50} was determined by plotting the logarithm of the drug concentration versus the survival rate of the treated cells.

Daunorubicin (DNR) accumulation

The accumulation into cells of DNR, a fluorescent compound, was studied by flow cytometry, as has been previously described.[17] Briefly, cells were incubated in the presence or absence of DPV576 (2.5%–10% v/v) at 37°C for 15 minutes. DNR (2 μM) was then added to the cells, gently mixed, and incubated at 37°C for 45 minutes. Accumulation of DNR was measured by flow cytometry using a FACScan (Becton Dickinson, Franklin Lakes, NJ, USA), the fluorescence intensity was recorded from histograms, and the data was expressed as mean fluorescence channel numbers (MFC).

AFM imaging

HL60/AR cells (0.5×10^6) were cultured with DPV576 (10% v/v) for 24 hours then exposed to DNR (2 μM) for 45 minutes. Results were compared to those of cells treated with DNR alone and DPV576 alone. Cytospin preparations (Shandon Southern Institute, Sewickley, PA, USA) of cells under different treatment conditions were air dried, fixed in 100% MeOH for 5 minutes, and prepared for AFM studies. Dimension 5000 AFM (Veeco, Plainview, NY, USA) under contact mode was used to image the HL60/AR cells with OTESP silicon probes (Veeco). Topographic height images were recorded at 512×512 pixels at a scan rate of 0.8 Hz. Image processing was performed using SPIP Software (Image Metrology, Hørsholm, Denmark). Usually an MLCT-AFM tip (with a 'k' value of 0.03 N/m) contributes to the broadening effect because of its specific geometry.[23]

Confocal imaging

Confocal laser scanning microscopy (CLSM) was used to detect DNR accumulation for HL60/AR cells treated with DNR alone and DNR plus DPV576. Cytospin preparations, as mentioned above, were prepared for confocal imaging.

The CLSM was operated in reflectance mode using a 515 nm laser line.[24]

Hole/vacuole analysis using light microscopy of Giemsa-stained preparations

Morphological assessment of hole induction in HL60/AR cells by DPV576 treatment was conducted in Giemsa-stained cytospin preparations. HL60/AR cells (0.5×10^6) were cultured with DPV576 (10% v/v) for 24 hours then exposed to DNR (2 μM) for 45 minutes. The cells (0.3×10^5) were then treated with either DPV576, DNR, DPV576 plus DNR, or saline. Afterwards, the samples were centrifuged on slides at 200 *g* for 5 minutes using a cytospin cytocentrifuge. Slides were air dried, fixed in 100% MeOH for 5 minutes, and then stained with 4% Giemsa solution for 15 minutes as has been previously described.[25]

Statistical analysis

Statistical significance was determined by Student's *t*-test. Differences were considered significant at the $P < 0.05$ level.

Results

The effects of DPV576 on the susceptibility of HL60/AR cancer cells to DNR were examined at the levels of both cell survival and drug accumulation.

HL60/AR cell survival

HL60/AR cells were cultured with DNR at different concentrations (1×10^{-9}–1×10^{-6} M) in the presence or absence of DPV576 for 3 days. Cell survival and IC_{50} values were then determined by MTT assay. Figure 1 shows that DNR, as expected, inhibited the survival of cancer cells in a dose-dependent manner and that the IC_{50} of DNR alone was 3.1 μM. However, when the cells were co-cultured with DPV576 plus DNR, we noticed a decrease in cell survival that was also dose dependent of DPV576 and maximized at 10% v/v. Subsequently, the IC_{50} was significantly reduced, reaching 0.8 μM at 10% v/v.

Drug accumulation

Flow cytometry

To determine if the observed DPV576-enhanced accumulation of DNR cytotoxicity in HL60/AR cells is related to an alteration in drug transport, we studied accumulation of DNR by flow cytometry. The results show that DPV576 at concentrations of 2.5%, 5%, and 10% v/v significantly enhances the accumulation of DNR in HL60/AR cells (Figure 2A and C). On the other hand, HL60 cells did not show changes in drug accumulation post-treatment with DPV576 and DNR (Figure 2B), suggesting that DPV576 had no significant effect on the accumulation of DNR in HL60 cells.

Confocal studies

HL60/AR cells treated with DNR in the presence and absence of DPV576 were examined by CLSM. Cells exposed to low concentrations of DNR alone showed very faint brightness (Figure 3A); similarly, cells treated with low and high doses of DNR also showed a faint brightness (Figure 3B and C).

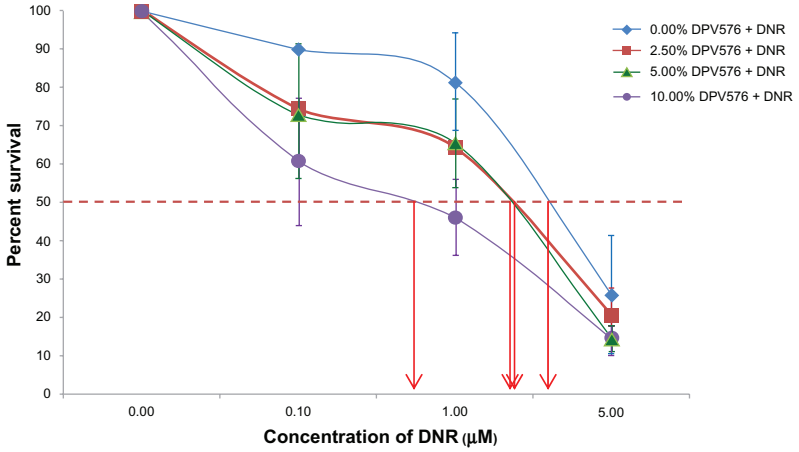

Figure 1 Effect of DPV576 on the reversal of DNR resistance in HL60/AR cells. Cancer cells (1×10^4 well^{-1}) were seeded in 96-well plates with DNR (1×10^{-9} to 1×10^{-6} M) and cultured in the presence or absence of various concentrations of DPV576 (2.5, 5, and 10% v/v) for 3 days. Cell survival was determined by MTT assay. Data represents the mean ± SD from three individual experiments, each in triplicate. The IC_{50} of DNR with DPV576 required 1/4th the amount of DNR as compared to the IC_{50} of DNR alone.
Abbreviations: DNR, daunorubicin; MTT, 3-[4,5-dimethylthiazol-2-yl]-2,5-diphenyltetrazolium bromide; IC_{50}, 50% inhibitory concentration.

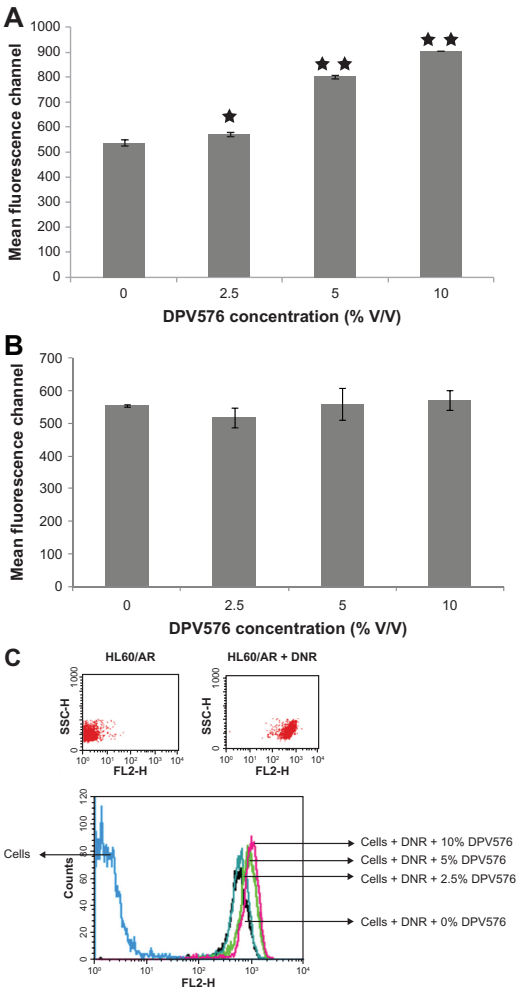

Figure 2 Effect of DPV576 on DNR accumulation in HL60/AR and HL60 cells using flow cytometry. Cancer cells (1×10^4) were incubated with DNR (2 μm) with or without DPV576 (2.5, 5, and 10% v/v) and drug accumulation was assessed using flow cytometry, and is expressed as MFC number. (**A**) HL60/AR cells; (**B**) HL60 cells; (**C**) dot plot and histogram overlays of HL60/AR cells with and without DNR and DPV576. Forward and side scatter was used to exclude debris and dead cells.
Notes: Data represent the mean ± SD of three experiments; $*P < 0.05$; $**P < 0.001$. Ten thousand cells were acquired for analysis by flow cytometry.
Abbreviations: DNR, daunorubicin; MFC, mean fluorescence channel.

On the other hand, cells exposed to high concentrations of DNR with DPV576 (Figure 3D–H) showed the greatest degree of brightness. Note the presence of multiple holes in these cells. Note also the apoptotic HL60/AR cells as characterized by an increased nuclear to cytoplasmic ratio in the early stages of apoptosis (Figure 3D–F) and membrane blebbing in the later stages of apoptosis (Figure 3G and H).

AFM studies

AFM studies were carried out to examine the hole formation in HL60/AR cells treated with DNR in the presence or absence of DPV576. Results show that hole formation is detected in the control (Figure 4A) and in DNR only treated cells (Figure 4B). However, hole formation is increased

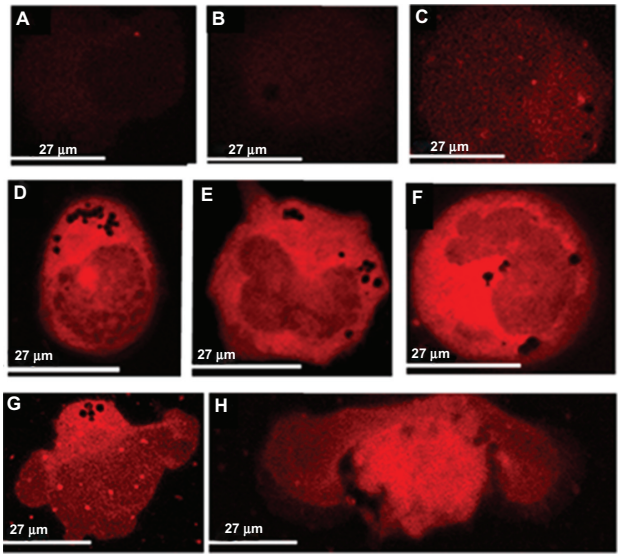

Figure 3 Effect of DPV576 on DNR accumulation in HL60/AR cells using CLSM. Cells displayed little to no brightness as shown in (**A**) without DNR and without DPV576, (**B**) cells with only DPV576, and (**C**) DNR alone. Cells exposed to both DNR and DPV576 show the highest degree of brightness (**D–H**). Note the increased degree of brightness in all of these co-treated cells. Also note the normal nuclear to cytoplasmic ratio in (**D**), increased ratio in (**E**), and further increased ratio in (**F**). Figure 3 also shows apoptotic HL60/AR cells. Note the cells with prominent membrane blebbing (**G** and **H**).
Abbreviations: CLSM, confocal laser scanning microscopy; DNR, daunorubicin.

post-treatment with DPV576 (Figure 4C). On the other hand, for HL60/AR cells treated with DNR plus DPV576, AFM detected marked increases in the size and number of holes (Figure 4D–I). These holes ranged from 40–500 nm in depth, and 0.1–2.5 μm in diameter, and were situated in the cytoplasm and the nucleus. Contrast images of Figures 4D and 4E correspond to Figure 4G and H and regions in dark orange indicate the depth of the holes. Figure 4I shows an apoptotic HL60/AR cell with membrane blebbing.

Discussion

Several studies have shown promising results for the role of nanoparticles in the reversal of chemo/radio-sensitization in cancer cells. Nanoparticles loaded with chemotherapeutic drugs have been used to successfully deliver drugs to the cytoplasm, nucleus, and other specific organelles.[26–28] For example, DNR-loaded magnetic nanoparticles of Fe_3O_4 can overcome MDR.[29] In another study, nickel nanoparticles have shown increased cancer cell membrane permeability.[7] However, the use of nanoparticles as DNR sensitizers has been of major concern due to their known toxicity. Exposure by inhalation to fine-grained nickel nanoparticles can cause cancer formation,[30] illness, and in some cases, death.[31] Cobalt nanoparticles have also been shown to display similar levels of toxicity[32] and tumor formation.[33]

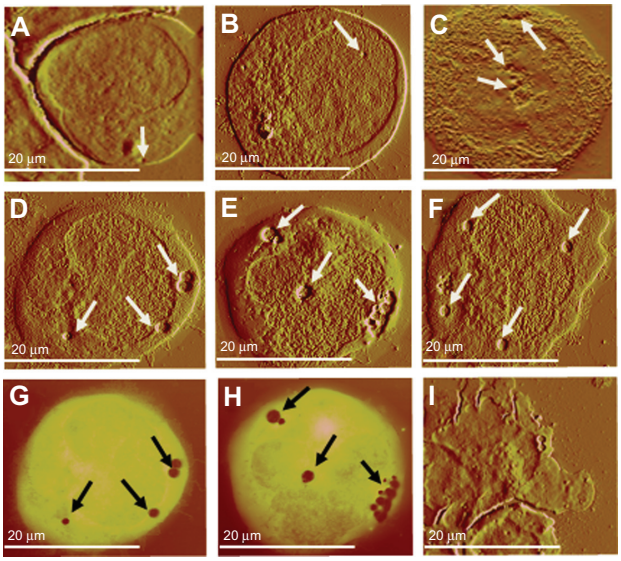

Figure 4 HL60/AR cells were cultured with DPV576 (10% V/V) for 24 hours then exposed to DNR (2 µM) for 45 minutes. Cytospin preparations of cells under different treatment conditions were air dried, fixed in MeOH, and prepared for AFM studies. Preparation showed no significant changes in hole formation in control cells untreated with DNR and DPV576 (**A**) and DNR only treated (**B**). DPV576 only treated (**C**) showed an increase in the number of holes. Preparation of DPV576 plus DNR treated cells (**D**–**F**) showed more frequent and larger-sized holes (white arrows). Contrast images of (**D** and **E**) correspond to (**G** and **H**), respectively, and regions in dark orange indicate the depth of the holes (black arrows). Finally, (**I**) shows an apoptotic cancer cell with signs of membrane blebbing.
Abbreviations: AFM, atomic force microscopy; DNR, daunorubicin.

Unlike other nanoparticles, DPV576 exhibits low levels of toxicity and yet reverses MDR in HL60/AR cells. Our preliminary results showed that DPV576 is less toxic as demonstrated by its ability to enhance human T cell and B cell proliferation in vitro (data not shown). Further studies by Schrand et al reported that NDs are non-toxic to a variety of cell types and did not produce significant reactive oxygen species.[34] In addition, the intratracheally instilled NDs showed no significant adverse effects in the lungs of mice as evaluated through histopathological and ultrastructural examinations.[35] Further studies suggest that NDs may have several biomedical applications due to their unique properties such as large specific surface areas, stable photoluminescence, and ability to be functionalized with biomolecules.[36,37] Moreover, DPV576 has shown immune modulatory effects such as activation of human monocyte-derived dendritic cells[21] and modulation of murine T lymphocytes by a mixture of ND/NP coated onto fabrics (DPV576-C) in mice.[22] In addition, results of the current study show that DPV576 reverses MDR in HL60/AR by a mechanism that involves hole induction.

The mechanisms of MDR in cancer cells have been the focus of research. These include a decreased uptake of hydrophilic drugs which require transporters to enter cells and an increased energy-dependent efflux of hydrophobic drugs that can enter cancer cells through the plasma membrane by diffusion. Other factors to be considered in reversing MDR include the decreased sensitivity to drug-induced apoptosis and induction of drug-detoxifying mechanisms.[38,39] In the last four decades, several attempts have been made to reverse MDR in MRP, and several chemosensitizers have been developed. These include: probenecid,[17] genistein,[18] buthionine sulfoximine,[19] ethacrynic acid, and calcium channel blockers.[20] In addition, hole induction by several nanoparticles represents an additional mechanism for reversing MDR.[7]

Our results indicate that DPV576 is an effective agent in the reversal of MDR as exemplified by the reduction of the IC_{50} to 1/4th upon exposure to DPV576. We identified via flow cytometry an increased accumulation of DNR in HL60/AR cells that was associated with the presence of several holes. The ability of different nanoparticles to induce holes has been reported in several types of cells. These include: transient holes caused by exposure of the cell membrane to monolayered protected nanoparticles;[40] cationic nanoparticles and macromolecules that generate transient holes in several biological membranes;[41] and an amine-modified nanoparticle treatment which resulted in hole induction in transformed human alveolar epithelial type 1-like cells.[42] The idea that such nanoparticles have the ability to alter the permeability of the respective cell membrane and thus facilitate the relevant drug uptake is very significant.

The observation of the hole-inducing capabilities of DPV576 may represent a possible mechanism by which this agent reverses MDR. Cancer cells have been shown to phagocytize microorganisms and other cells, and subsequently, vacuoles can be seen in these cancer cells. Many tumor cells exhibit phagocytic activity, including: phagocytosis of titanium particles by sarcoma L929 cells;[43] elastic fibers by dermatofibroma cells;[44] erythrocytes and bacteria by adenocarcinomas;[45,46] *Candida albicans* by lymphatic tumor cells;[47] and *Saccharomyces cerevisiae* by human breast, oral, and colon cancer cells.[48,49] Cancer cells can also phagocytize other cells such as lymphocytes[50,51] and neutrophils.[52] In addition, phagocytosis of one tumor cell by another tumor cell has been reported[53] and is referred to as cannibalism. In the current study, we detected the presence of holes in the control untreated HL60/AR cells (Figure 4A) via AFM, which may be attributed to their cannibalistic activity. Treatment with DPV576 increased hole formation in cells (Figure 4C) and showed a three-fold increase in the percentage of cells with multiple holes (≥4) as compared to control untreated cells (Figure 4A) and DNR only treated

cells (Figure 4B). However, HL60/AR cells co-treated with DPV576 plus DNR showed holes more frequent in number and which appeared larger in size, ranging from 40–500 nm in depth and 0.1–2.5 μm in diameter, and were situated in the cytoplasm and the nucleus (Figure 4D–I). AFM studies were further confirmed using CLSM imaging.

Another mechanism by which DPV576 might kill HL60/AR cells is through interference with MRP and drug transport via modulation of the transport function of MRP. MRP is a member of the ATP-binding cassette superfamily of membrane transport proteins and has been suggested to play a role in the reduction of drug accumulation.[19] Normally, MDR cells overexpress P-glycoproteins (P-gp); using a nanoformulation of drugs is one way of bypassing the P-gp pumps. Since HL60/AR is a cell line that is known to overexpress MRP,[17] the data suggests that DPV576 might induce HL60/AR cell apoptosis through interference with drug transport in addition to inducing holes in the cancer cell membrane.

Several studies suggest that DPV576 serves a dual purpose in the fight against cancer – in addition to its ability to induce holes in cancer cells, it has been shown to have an immune modulatory effect.[21,22] Such properties of DPV576 make this agent advantageous over other nanoparticles.

Conclusion

This study strongly suggests that DPV576 reverses resistance in HL60/AR cells by increasing cellular DNR accumulation via a mechanism that may involve induction of holes in the cellular membrane. It should be investigated as a unique candidate for drug delivery and MDR therapy with less toxic effects.

Acknowledgments

The authors are greatly indebted to Dr Sastry Gollapudi, Professor of Immunology, Division of Basic and Clinical Immunology, University of California, Irvine, CA, USA, for assistance in revision of the manuscript. The authors would also like to thank Venex Company, Atsugi, Kanagawa, Japan, for providing DPV576. Confocal laser scanning microscope work was performed at the California Nanosystems Institute Advanced Light Microscopy/Spectroscopy Shared Resource Facility at the University of California, Los Angeles, supported with funding from the National Institutes of Health – National Center for Research Resources shared resources grant (CJX1-443835-WS-29646) and the National Science Foundation Major Research Instrumentation grant (CHE-0722519). Atomic force microscopy imaging was performed at Nano and Pico Characterization Lab at the California Nanosystems Institute.

Disclosure

The authors report no conflicts of interest in this work.

References

1. Lu J, Liong M, Sherman S, et al. Mesoporous silica nanoparticles for cancer therapy: energy-dependent cellular uptake and delivery of paclitaxel to cancer cells. *Nanobiotechnology*. 2007;3(2):89–95.
2. Anhorn MG, Wagner S, Kreuter J, Langer K, von Briesen H. Specific targeting of HER2 overexpressing breast cancer cells with doxorubicin loaded trastuzumab-modified human serum albumin nanoparticles. *Bioconjug Chem*. 2008;19(12):2321–2331.
3. Yousefpour P, Atyabi F, Vasheghani-Farahani E, Movahedi AA, Dinarvand R. Targeted delivery of doxorubicin-utilizing chitosan nanoparticles surface-functionalized with anti-Her2 trastuzumab. *Int J Nanomedicine*. 2011;6:1977–1990.
4. Chen T, Cheng T, Chen C, et al. Targeted Herceptin-dextran iron oxide nanoparticles for noninvasive imaging of HER2/neu receptors using MRI. *J Biol Inorg Chem*. 2009;14(2):253–260.
5. Sun B, Ranganathan B, Feng SS. Multifunctional poly (D,L-lactide-coglycolide)/montmorillonite (PLGA/MMT) nanoparticles decorated by Trastuzumab for targeted chemotherapy of breast cancer. *Biomaterials*. 2008;29(4):475–486.
6. Cirstoiu-Hapca A, Bossy-Nobs L, Buchegger F, Gurny R, Delie F. Differential tumor cell targeting of anti-HER2 (Herceptin®) and anti-CD20 (Mabthera®) coupled nanoparticles. *Int J Pharm*. 2007;331(2):190–196.
7. Guo D, Wu C, Li J, et al. Synergistic effect of functionalized nickel nanoparticles and Quercetin on inhibition of the SMMC-7721 cells proliferation. *Nanoscale Res Lett*. 2009;4(12):1395–1402.
8. Steinhauser I, Spänkuch B, Strebhardt K, Langer K. Trastuzumab modified nanoparticles: optimisation of preparation and uptake in cancer cells. *Biomaterials*. 2006;27(28):4975–4983.
9. Steinhauser IM, Langer K, Strebhardt KM, Spänkuch B. Effect of trastuzumab-modified antisense oligonucleotide-loaded human serum albumin nanoparticles prepared by heat denaturation. *Biomaterials*. 2008;29(29):4022–4028.
10. Sharma S, Santiskulvong C, Bentolila LA, Rao J, Dorigo O, Gimzewski JK. Correlative nanomechanical profiling with super-resolution F-actin imaging reveals novel insights into mechanisms of cisplatin resistance in ovarian cancer cells. *Nanomedicine*. 2012;8(5):757–766.
11. Singal PK, Iliskovic N. Doxorubicin-induced cardiomyopathy. *N Engl J Med*. 1999;339(13):900–905.
12. Francis PA, Kris MG, Rigas JR, Grant SC, Miller VA. Paclitaxel (Taxol) and docetaxel (Taxotere): active chemotherapeutic agents in lung cancer. *Lung Cancer*. 1995;1:S163–S172.
13. Fossella FV, Lee JS, Berille J, Hong WK. Summary of phase II data of docetaxel (Taxotere), an active agent in the first- and second-line treatment of advanced non-small cell lung cancer. *Semin Oncol*. 1995;22(2):22–29.
14. Strauss GM, Lynch TJ, Elias AD, et al. A phase I study of ifosfamide/carboplatin/etoposide/paclitaxel in advanced lung cancer. *Semin Oncol*. 1995;22(4):70–74.
15. Sanderson BJ, Ferguson LR, Denny WA. Mutagenic and carcinogenic properties of platinum-based anticancer drugs. *Mutat Res*. 1996;355(1–2):59–70.
16. Santin AD, Hermonat PL, Ravaggi A, et al. Effects of concurrent cisplatinum administration during radiotherapy vs radiotherapy alone on the immune function of patients with cancer of the uterine cervix. *Int J Radiat Oncol Biol Phys*. 2000;48(4):997–1006.
17. Gollapudi S, Kim CH, Tran BN, Sangha S, Gupta S. Probenecid reverses multidrug resistance in multidrug resistance-associated protein-overexpressing HL60/AR and H69/AR cells but not in P-glycoprotein-overexpressing HL60/Tax and P388/ADR cells. *Cancer Chemother Pharmacol*. 1997;40(2):150–158.

18. Versantvoort CH, Schuurhuis GJ, Pinedo HM, et al. Genistein modulates the decreased drug accumulation in non-P-glycoprotein mediated multidrug resistant tumour cells. *Br J Cancer*. 1993;68(5):939–946.
19. Chuman Y, Chen ZS, Seto K, et al. Reversal of MRP-mediated vincristine resistance in KB cells by buthionine sulfoximine in combination with PAK-104P. *Cancer Lett*. 1998;129(1):69–76.
20. Phillips PC. Antineoplastic drug resistance in brain tumors. *Neurol Clin*. 1991;9(2):383–404.
21. Ghoneum M, Ghoneum A, Gimzewski J. Nanodiamond and nanoplatinum liquid, DPV576, activates human monocyte-derived dendritic cells in vitro. *Anticancer Res*. 2010;30(10):4075–4079.
22. Ghoneum M, Ghoneum A, Tolentino L, Gimzewski J. Modulation of aged murine T lymphocytes in vivo by DPV576-C, a nanodiamond- and nanoplatinum-coated material. *In Vivo*. 2010;24(2):141–146.
23. Sharma S, Rasool HI, Palanisamy V, et al. Structural-mechanical characterization of nanoparticle exosomes in human saliva, using correlative AFM, FESEM, and force spectroscopy. *ACS Nano*. 2010;4(4):1921–1926.
24. Petrou I, Heu R, Stranick M, et al. A breakthrough therapy for dentin hypersensitivity: how dental products containing 8% arginine and calcium carbonate work to deliver effective relief of sensitive teeth. *J Clin Dent*. 2009;20(1):23–31.
25. Kumagai K, Itoh K, Suzuki R, Hinuma S, Saitoh F. Studies of murine large granular lymphocytes. I. Identification as effector cells in NK and K cytotoxicities. *J Immunol*. 1982;129(1):388–394.
26. Allen TM, Cullis PR. Drug delivery systems: Entering the mainstream. *Science*. 2004;303:1818–1822.
27. Choleris E, Little SR, Mong JA, Puram SV, Langer R, Pfaff DW. Microparticle-based delivery of oxytocin receptor antisense DNA in the medial amygdala blocks social recognition in female mice. *Proc Natl Acad Sci U S A*. 2007;104:4670–4675.
28. Misra R, Sahoo SK. Coformulation of doxorubicin and curcumin in poly(D,L-lactide-co-glycolide) nanoparticles suppresses the development of multidrug resistance in K562 cells. *Mol Pharm*. 2011;8(3):852–866.
29. Chen BA, Lai BB, Cheng J, et al. Daunorubicin-loaded magnetic nanoparticles of Fe3O4 overcome multidrug resistance and induce apoptosis of K562-n/VCR cells in vivo. *Int J Nanomedicine*. 2009;4: 201–208.
30. Sano N, Shibata M, Izumi K, Otsuka H. Histopathological and immunohistochemical studies on nickel sulfide-induced tumors in F344 rats. *Jpn J Cancer Res*. 1988;79:212–221.
31. Phillips JI, Green FY, Davies JC, Murray J. Pulmonary and systemic toxicity following exposure to nickel nanoparticle. *Am J Ind Med*. 2010;53:763–767.
32. Lison D, De Boeck M, Verougstraete V, Kirsch-Volders M. Update on the genotoxicity and carcinogenicity of cobalt compounds. *Occup Environ Med*. 2001;58:619–662.
33. Hansen T, Clermont G, Alves A, et al. Biological tolerance of different materials in bulk and nanoparticulate form in a rat model: sarcoma development by nanoparticles. *J R Soc Interface*. 2006;3(11): 767–775.
34. Schrand AM, Huang H, Carlson C, et al. Are diamond nanoparticles cytotoxic? *J Phys Chem B*. 2007;111(1):2–7.
35. Yuan Y, Wang X, Jia G, et al. Pulmonary toxicity and translocation of nanodiamond in mice. *Diam Relat Mater*. 2010;19:291–299.
36. Xing Y, Dai L. Nanodiamonds for nanomedicine. *Nanomedicine*. 2009;4(2):207–218.
37. Mochalin VN, Shenderova O, Ho D, Gogotsi Y. The properties and applications of nanodiamonds. *Nat Nanotechnol*. 2011;7(1):11–23.
38. Szakács G, Paterson JK, Ludwig JA, Booth-Genthe C, Gottesman MM. Targeting multidrug resistance in cancer. *Nat Rev Drug Discov*. 2006;5(3):219–234.
39. Gottesman MM. Mechanisms of cancer drug resistance. *Annu Rev Med*. 2002;53:615–627.
40. Verma A, Uzun O, Hu Y, et al. Surface structure-regulated cell membrane penetration by monolayer protected nanoparticles. *Nat Mater*. 2008;7(7):588–595.
41. Leroueil PR, Hong SY, Mecke A, Baker JR, Orr BG, Holl MM. Nanoparticle interaction with biological membranes: Does nanotechnology present a janus face? *Accounts Chem Res*. 2007;40:335–342.
42. Ruenraroengsak P, Novak P, Berhanu D, et al. Respiratory epithelial cytotoxicity and membrane damage (holes) caused by amine-modified nanoparticles. *Nanotoxicology*. 2012;6(1):94–108.
43. Osano E, Kishi J, Takahashi Y. Phagocytosis of titanium particles and necrosis in TNF-alpha resistant mouse sarcoma L929 cells. *Toxicol In Vitro*. 2003;17(1):41–47.
44. Kiyohara T, Kumakiri M, Kobayashi H, Ohkawara A, Lao LM. Atrophic dermatofibroma. Elastophagocytosis by the tumor cells. *J Cutan Pathol*. 2000;27(6):312–315.
45. Marin-Padilla M. Erythrophagocytosis by epithelial cells of a breast carcinoma. *Cancer*. 1977;39(3):1085–1089.
46. Vandenberghe J, Verheyen A, Lauwers S, Geboes K. Spontaneous adenocarcinoma of the ascending colon in Wistar rats: the intracytoplasmic presence of a Campylobacter-like bacterium. *J Comp Pathol*. 1985;95(1):45–55.
47. Ghoneum M, Grewal I, Brown J, Osborne R, Elembabi H, Gill G. Phagocytosis of candida albicans by lymphatic tumour cells in vitro. *Acta Histochem*. 2003;105(2):127–133.
48. Ghoneum M, Gollapudi S. Phagocytosis of Candida albicans by metastatic and non metastatic human breast cancer cell lines in vitro. *Cancer Detect Prev*. 2004;28(1):17–26.
49. Ghoneum M, Hamilton J, Brown J, Gollapudi S. Human squamous cell carcinoma of the tongue and colon undergoes apoptosis upon phagocytosis of Saccharomyces cerevisiae, the baker's yeast, in vitro. *Anticancer Res*. 2005;25(2A):981–989.
50. Ghoneum M, Salem F, Shum SS, Perry L, Gill G. In situ lymphophagocytosis by nonlymphoreticular neoplasms. *Nat Immun Cell Growth Regul*. 1987;6(2):77–87.
51. Ghoneum M, Salem F, Allen H, Gill G. Phagocytosis of autologous lymphocytes by cervical preneoplastic and neoplastic cells. *Nat Immun Cell Growth Regul*. 1988;7(4):239–248.
52. Singhal N, Handa U, Bansal C, Mohan H. Neutrophil phagocytosis by tumor cells – a cytological study. *Diagn Cytopathol*. 2011;39(8): 553–555.
53. Overholtzer M, Mailleux AA, Mouneimne G, et al. A nonapoptotic cell death process, entosis, that occurs by cell-in-cell invasion. *Cell*. 2007;131(5):966–979.